JOURNAL OF MATERIALS SCIENCE **36** (2001) 5845–5851

Diffusion barrier properties of ionized metal plasma deposited tantalum nitride thin films between copper and silicon dioxide

KHIN MAUNG LATT, Y. K. LEE
School of Materials Engineering, Nanyang Technological University, Nanyang Avenue, Singapore 639798
E-mail: p101282@ntu.edu.sg

H. L. SENG, T. OSIPOWICZ
Department of Physics, National University of Singapore, Lower Kent Ridge Road, Singapore 119260

Tantalum nitride thin films with different thickness are sputtered deposited on silicon dioxide in the Cu/TaN/SiO_2/Si multiplayer structure. Using resistivity analyses, X-ray diffraction, scanning electron microscopy and Rutherford backscattering spectroscopy, this work examines the impact of varying layer thickness on the crystal structure, resistivity, intermixing and reactions at the interfaces before and after annealing. The thinner the film thickness of TaN, the severe the reactions at the interface of Cu/TaN and consumed more conductive Cu. All the structures shown similar degradation process, and were found to be stable up to 500°C for 35 min. Accelerated grain growth and agglomeration were also observed after annealing temperature higher than 550°C at all Cu surfaces of the samples.

1. Introduction

The current trend in shrinking integrated circuits to increase the logical density and improve the performance of chip requires substituting copper for aluminium as interconnects in the deep submicron integrated circuits. This trend is reinforced by the fact that Cu offers lower resistivity and superior electromigration and stress-voiding resistance over Al and its alloys [1]. However, several Cu-related problems, including high mobility, strong reactivity, and poor adhesion, should be first solved in order to fully integrated Cu into the integrated circuits. The successful implementation of Cu-based metallization for ULSI Si devices requires not only new manufacturing technologies and design modifications but also a new material systems that act as effective diffusion barriers, protection layers, adhesion promoters low-k dielectric. Electrical and structural properties of Ta thin films have received considerable attention owing to their widespread applications in electronic devices and X-ray lithography [2–4]. Since the advent of Cu interconnects for deep submicron multilevel integrated circuits, Ta is a highly promising polish stop and adhesion layer for chemical mechanical polishing (CMP) of damascence process [5]. Furthermore, as generally accepted, Ta and nitrogen-contained tantalum (Ta-N) thin films are the most promising diffusion barriers to prevent the highly diffusing Cu from reacting with the underlying silicon and surrounding SiO_2 dielectric [6–12]. Thus, the feasibility of growing Ta and TaN thin film has been extensively studied, particularly in terms of controlling the phase, electrical property and microstructure of the Ta and TaN films so that they can be used as reliable barriers between Cu and Si/SiO_2 and Cu [6–13].

Taking into consideration the further dimension decrease and the necessity of complete line encapsulating a thick barrier layer can significantly increase the net line resistance. Hence, the barrier thickness has to be adapted for each new generation according to the reliable and performance requirement. According to relationship between critical dimension and barrier thickness, for the dimensions below 0.18 μm the barrier thickness should be reduced down to 10 nm in order to achieve a gain in performance. Additionally, both increasing the aspect ratio of the vias and decreasing their cross section cause barrier thinning at via sidewalls and bottoms. The necessary reduction in barrier thickness places severe requirements on the barrier quality. In our present work, TaN diffusion barriers with difference thickness were deposited by Ionized Metal Plasma (IMP) sputtering. It will overcome the generic PVD processing limitations such as the poor step coverage without losing the excellent metallurgical diffusion barrier properties. In addition, IMP deposition makes the TaN film microstructure denser, in particular, in grain boundaries. Hence, the diffusion and intermixing of Cu through TaN film can be blocked effectively due to the discontinuous grain boundaries, which is expected to improve the barrier properties much better than reactive sputtered TaN. The test sample structure is Cu

(200 nm)/TaN (30, 20, 10 nm)/SiO_2 (250 nm)/Si and the diffusion barrier properties were evaluated by electrical measurement. Furthermore, XRD, AFM and RBS were employed in conjunction with electrical measurements to examine the failure mechanism.

In particular, a reliable and high conductive thin-film diffusion barrier of resistivity less than 300 $\mu\Omega$ cm and thickness less than 40 nm should be employed to effectively retard Cu from intermixing and reacting with Si. Indeed, the ability of a wide variety of transition metal-related thin film barrier materials for Cu has been extensively investigated.

2. Experimental details

For all sample preparation and experiments described in this study used 8″ Si (100) wafers. Si wafers were cleaned in 10 : 1 diluted HF solution and rinsed in deionized water before SiO_2 deposition. First, a 500 nm thick plasma enhanced chemical vapor deposited (PECVD) SiO_2 dielectric was deposited by using a gas mixture of SiH_4, O_2 and Ar at 400°C on 8″ Si wafers. Tantalum nitride (TaN) films of different thickness, 30 nm (sample **A**), 20 nm (sample **B**), and 10 nm (sample **C**) which act as a diffusion barrier and adhesion layer for the highly conductive Cu atoms, were deposited onto PECVD-SiO_2 (500 nm)/Si substrates by using ionized metal plasma (IMP) sputtering in a gas mixture of Ar and N_2. Without breaking the vacuum, a 200 nm Cu layer was then deposited by IMP sputtering. Detailed IMP deposition process has been described elsewhere [13]. The Cu/TaN/SiO_2/Si multiplayer structure samples were then annealed for 35 min in a programmable furnace under the protection of nitrogen ambient at the temperatures ranging from 350 to 650°C. The sheet resistance measurement of the multilayer structure samples before and after annealing were measured by four-point probe (Tencor Flexus 2320) to survey the overall reactions involving Cu. The surface morphologies of the structure at various temperatures were observed by JEOL 5410 Scanning Electron Microscope (SEM) employing a 20 KeV primary electron beam. The X-ray diffraction (XRD) measurements were performed with a RIGAKU model RINT2000 diffractometer using a $\gamma = 2.5^\circ$ grazing incident angle geometry. The Cu K_α X-ray ($\lambda = 1.542$ Å at 50 KV and 20 mA) detection was done from $2\theta = 10^\circ$ to $2\theta = 90^\circ$ with scan speed of 1°/min and scan step 0.05° for the analysis of reaction product phases and the interdiffusion of the elements across the interface, respectively. RBS spectra were taken with 2 MeV He^+ ions at a scattering angle of 160° using a 50 mm^2 Passivated Implanted Planar Silicon (PIPS) detector of 14 KeV resolution.

3. Results and discussion

Fig. 1 show the SEM micrograph and XRD scan for as deposited TaN film used in this experiment. It can be clearly seen that TaN film is composed of very fine grains (nanostructure and/or amorphous) and diffraction pattern of the film contains two broad low intensity peaks having a full width at half maximum of 6° (second peak). This observation implied that this TaN film is constituted mainly of an amorphous phase material. Notably, two different phases, such as amorphous and crystalline Ta_2N, or Ta_2N and TaN, can coexist within the limited range of N_2 flow rates [11, 14]. Regardless of the thickness the microstructure of as deposited TaN (sample **A**, **B**, and **C**) films were found to be the same. The resistivity of the as-prepared films also examined by measuring the sheet resistance using four-point probe method. The as deposited films (sample **A**, **B**, and **C**) show a value of ~200 $\mu\Omega$ cm, which agrees well with the minimum value of the resistivity of the TaN compound reported by Hieber [15]. The Cu films on respective TaN film thickness also have a predominantly (220) texture (sample **A**, **B**, and **C**). Assuming the broad peak in FWHM is due to the fine grains in the films, the grain sizes of the as deposited films are about 80 Å as estimated from the widths of the reflection lines. Although this result is only a roughly estimated one, but not directly confirmed, the qualitative tendency may be exact and also suggest that the obtained films of TaN consist of fine grains. This agree well with the report by Sun *et al.* [14] that the grains of the TaN crystalline phases are considerable small and their sizes decrease with the increasing N_2 concentration.

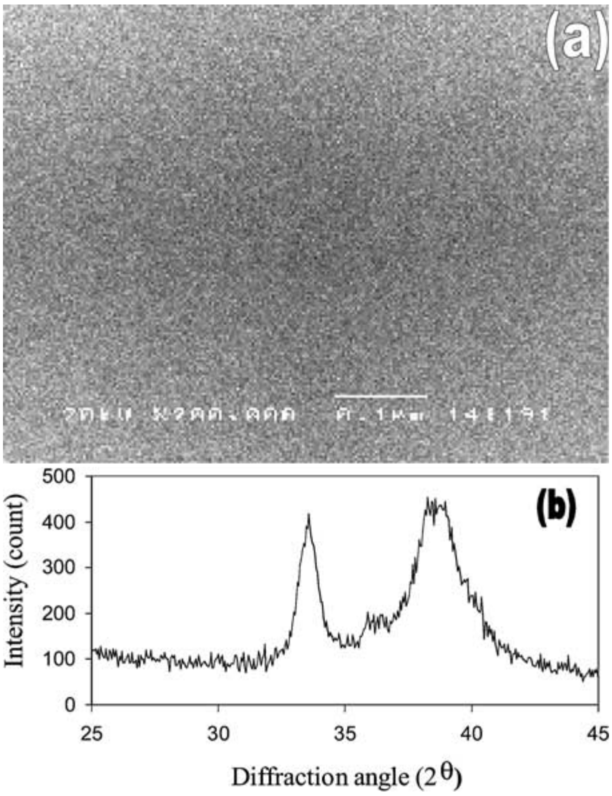

Figure 1 (a) SEM micrograph and, (b) XRD pattern of as deposited TaN showing nanocrystalline structure.

The graphs presented in Fig. 2 indicate the change in sheet resistance measured on the Cu/TaN/SiO_2/Si structure as a function of annealing temperature in N_2 ambient for 35 min. The measured sheet resistance was dominated by the Cu thin film since the copper film (200 nm and 1.72 $\mu\Omega$ cm) is much thicker and has a markedly lower resistivity than that of TaN films (10, 20, 30 nm and ~216 $\mu\Omega$ cm) and any reaction products.

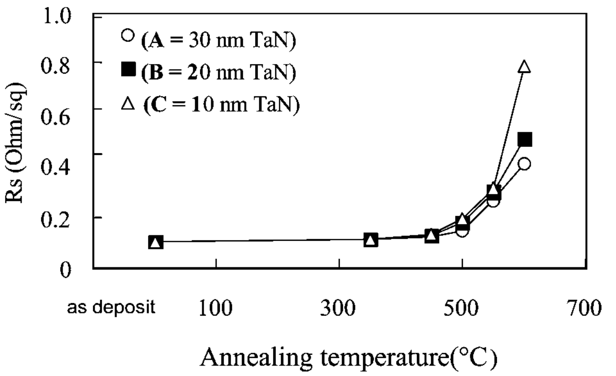

Figure 2 Sheet resistance of Cu/TaN/SiO_2/Si samples as a function of temperature.

Since the top Cu layer of 200 nm carries nearly all the sensor current, the sheet resistance measurements monitor the condition and the quality of the Cu overlayer. Hence, these curves can be used to estimate the degree of intermixing, reaction, and changes of integrity across the metallization layers as well. According to this figure, all samples, annealed up to 450°C can maintain the same level of sheet resistance as the as-deposited samples. However, the sheet resistance increases slightly at temperatures just exceeding 450°C, implying that a relatively resistive substance has been produced from the highly conductive Cu layers. As the temperature reaches 550°C and beyond, the sheet resistance of the samples rises abruptly, indicating that a severe intermixing or interfacial reactions occurred across all the Cu films.

To identify the new phases formed during the annealing, X-ray diffraction analysis (XRD) was carried out to evaluate the interaction between layers. Fig. 3 displays a typical series of XRD patterns for freshly prepared Cu/TaN/SiO_2/Si (sample **A** = 30 nm TaN) structures and annealed at temperatures ranging from 350°C to 650°C. The diffraction pattern reveals that the as-deposited TaN thin films indeed exhibit two broad low intensity peaks. Subsequently, after annealing 350°C and 450°C, these broad peaks are converted into a single sharp peak that reach saturated intensities and locate at the positions corresponding to hexagonal Ta_2N. This transformation suggests that the sputter deposited Ta_2N diffusion barriers are mainly amorphous/nanocrystalline, and can easily undergo a crystallization transition at temperatures as low as 450°C. This peak was overlapped by the Cu_2O peak, which starts forming at 450°C annealing. The intensities of the Cu (220) peak increase after annealing 350°C, presumably due to the annihilation of the inherent crystal defects and grain growth of the Cu layer. However, the intensities of this peak slightly decrease again as an annealing temperature surpasses 500°C. This suggests that some Cu atoms were consumed by forming Cu_2O. But the formation of Cu_2O at 2θ angles 36.35°(111), 42.36°(200) and 61.30°(220) become prominent as annealing temperature increase. After 650°C annealing, two peaks with very low intensity were found at 22.8° and 28.35° and they are identified as Ta_2O_5 and $Cu_xTa_yO_z$.

Another series of XRD patterns presented in Fig. 4 indicate that the Cu/TaN/SiO_2/Si (sample **B** = 20 nm TaN) structure follow a transition process similar to that of sample **A**. However, the intensities of Cu (220) peak decrease continuously as the annealing temperature surpasses 500°C. The intensity of Cu peak after 650°C was found to be very much less than that of in sample **A** and the peaks of new compounds were more visible compare to sample **A**. The diffraction pattern display in Fig. 5 clearly reveals that Cu peak (of sample **C** = 10 nm TaN) after annealing 650°C was significantly reduced and Ta_2O_5 and $Cu_xTa_yO_z$ peaks were stronger in intensity compared to both **A** and **B**. This observation leads to a conclusion that the thinner in Ta_2N barrier the more severe in the reaction between Cu and Ta_2N and consumed more conductive Cu layer which attributed the highest rise in R_s value for sample **C** in Fig. 2.

Here, three sources of oxygen atoms forming Cu_2O and Ta_2O_5 in all samples will be considered. Firstly, oxygen atoms from the SiO_2, which would diffuse into

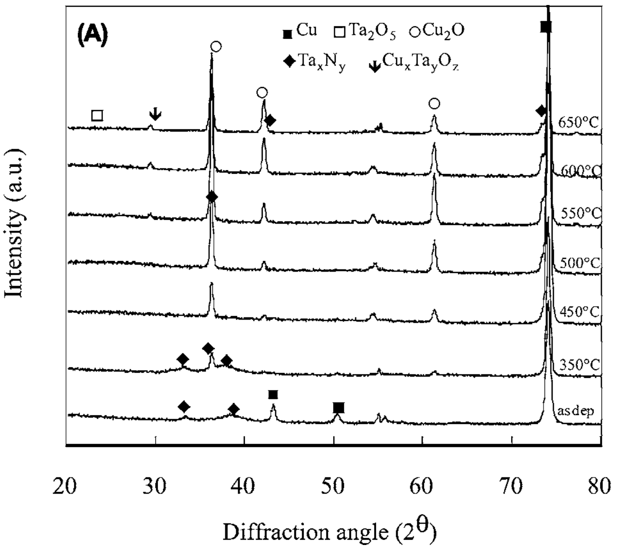

Figure 3 XRD patterns of the Cu/TaN (10 nm)/SiO_2/Si structure annealed at various temperatures for 35 min in N_2 ambient.

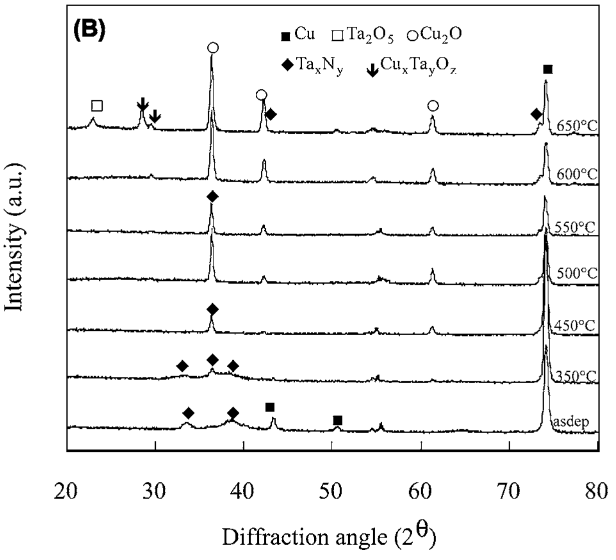

Figure 4 XRD patterns of the Cu/TaN (20 nm)/SiO_2/Si structure annealed at various temperatures for 35 min in N_2 ambient.

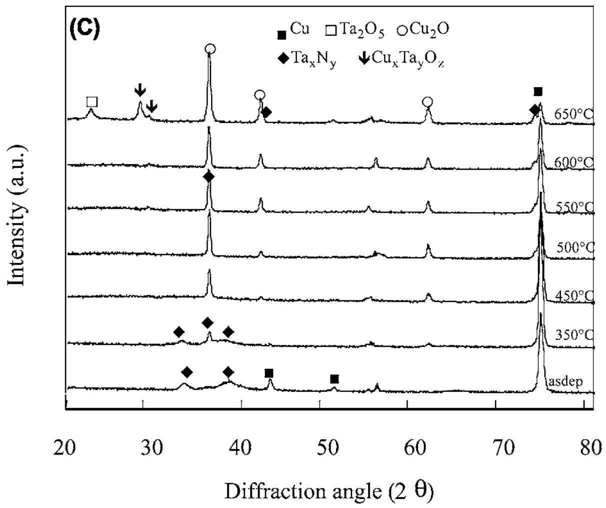

Figure 5 XRD patterns of the Cu/TaN (30 nm)/SiO_2/Si structure annealed at various temperatures for 35 min in N_2 ambient.

and/or react with the Ta_xN_y layer, as the annealing temperature increased since Lane *et al.* reported the possible reactions between SiO_2 and TaN and the formation of Ta_2O_5 [16]. The second source is oxygen atoms incorporated with Cu and Ta metal film from the deposition ambient during the Cu and Ta deposition and decorating the grain boundaries of each film [17]. We also reported the oxygen and carbon concentration and the depth profile in IMP-TaN and IMP-Cu, being examined by SIMS analysis and the formation of Cu_2O and Ta_2O_5 [18]. Lastly, oxygen atoms incorporated from annealing ambient, but were excluded because all the samples were annealed in an "inert" nitrogen atmosphere. However, the formation of Cu_2O and/or Ta_2O_5 cannot be fully prevented. This reveals the fact that formation of Cu_2O and Ta_2O_5 in the structure is mainly due to the oxygen incorporated during the deposition process and form SiO_2. The intensity of Cu (200) peak was slightly reduced due to the formation of Cu_2O. For the case of Ta_2O_5, according to the Ta-O binary system, up to approximately 30 at.% of the oxygen could be interstitially dissolved in the b.c.c-Ta lattice prior to conversion into the amorphous or polycrystalline Ta_2O_5 phase [19]. As impurity in polycrystalline Ta films, O is believed to increase the effectiveness of the diffusion barrier by decorating the extended defects such as grain boundaries, thereby blocking the active paths for grain boundary diffusion [7]. Annealing at temperatures higher than 450°C makes Cu and weakly bonded Ta_xN_y start to react with the O_2 existing in the grain boundaries of Cu as well as Ta_2N resulted in the formation of Cu_2O and Ta_2O_5. By annealing at 650°C, a new peak of $Cu_7Ta_{15}O_{41}$ appeared at 28.35°, probably due to the reaction among Cu_2O, Ta_2O_5, Ta and Cu at the interface of Cu/Ta_2N [20]. As a result, a reduced in intensity of Cu (220) and Ta_xN_y peaks was also observed due to the formation of Cu_2O, Ta_2O_5, and $Cu_7Ta_{15}O_{41}$. The peak of a new compound was observed very close to Ta_2O_5 peak. Although an interfacial reaction and the formation of Cu_2O, Ta_2O_5 occurred in the structure, no evidence of the diffusion of Cu through the barrier (copper silicide formation) was detected even after annealing at 650°C for 35 min. But the Cu peaks of the sample **B** and **C** were significantly reduced. In order to determined whether the diffusion of Cu through the barrier layer or not, the RBS analysis was performed.

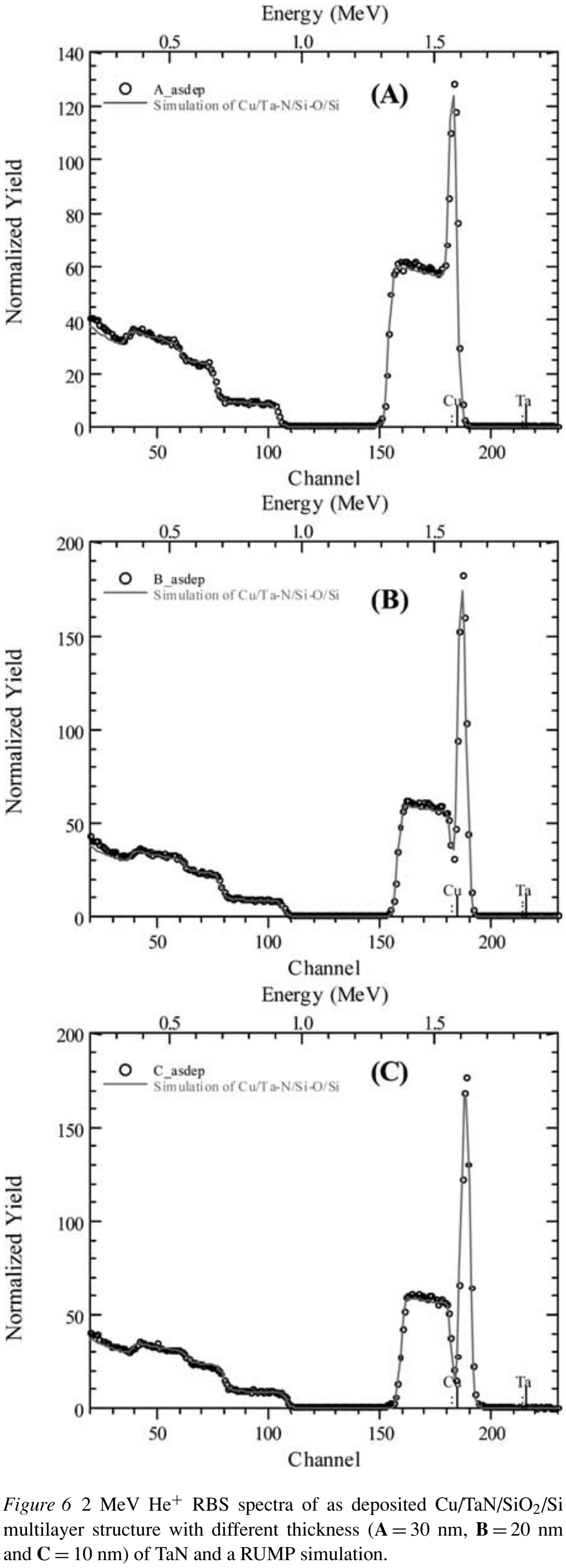

Figure 6 2 MeV He^+ RBS spectra of as deposited Cu/TaN/SiO_2/Si multilayer structure with different thickness (**A** = 30 nm, **B** = 20 nm and **C** = 10 nm) of TaN and a RUMP simulation.

Rutherford backscattering (RBS) measurements were performed to evaluate the interaction between the different layers. Fig. 6 shows both the experimental and the simulated RBS spectra of as deposited

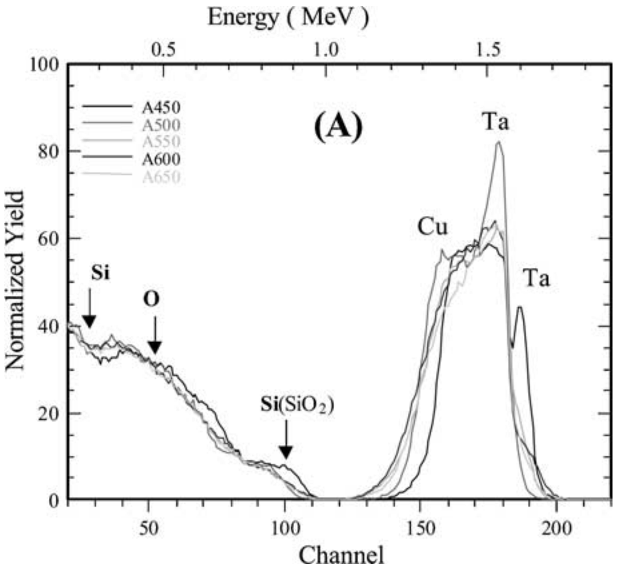

Figure 7 2 MeV He$^+$ RBS spectra of Cu/TaN/SiO$_2$/Si multilayer (**A** = 30 nm TaN) annealed at various temperatures.

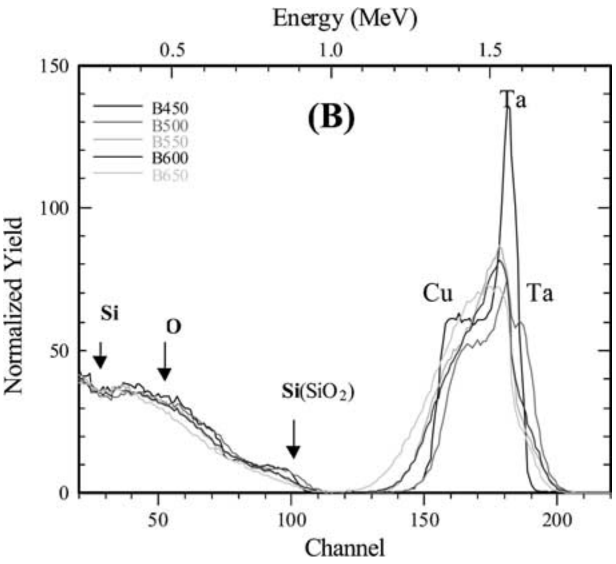

Figure 8 2 MeV He$^+$ RBS spectra of Cu/TaN/SiO$_2$/Si multilayer (**B** = 20 nm TaN) annealed at various temperatures.

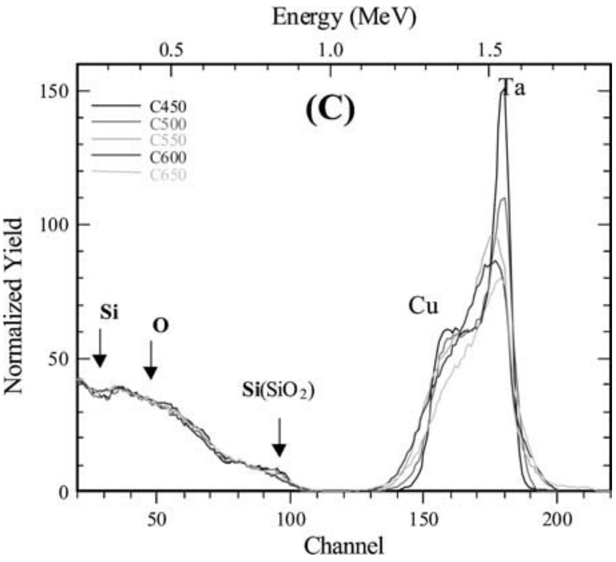

Figure 9 2 MeV He$^+$ RBS spectra of Cu/TaN/SiO$_2$/Si multilayer (**C** = 10 nm TaN) annealed at various temperatures.

Cu/TaN/SiO$_2$/Si structures for all the samples (**A**, **B**, **C**) with the surface energies of Cu and Ta indicated. Fig. 7 shows the RBS spectra of sample **A** annealed from 350 to 650°C for 35 min. At 350°C, the RBS spectrum shows sharp layer structures. At higher anneal temperature of 450°C, the Ta peak position for sample **A** shifts from 1.57 MeV to a higher energy at 1.60 MeV. This observation suggests either an out diffusion of Ta into the Cu film or a reduction in the Cu thickness. Nevertheless, the Cu surface seems to be free of Ta atoms since the energy of the Ta peak observed is lower than the Ta surface peak energy. It seems that the out diffusion of Ta atoms is mainly distributed within the Cu film grain boundaries. At 500°C, the Ta peaks were observed to have broadened and moved back to a lower energy. Tailing of the Cu peaks was observed at the low energy edge, which suggest the occurrence of agglomeration in the Cu layer. This is also confirmed by the SEM micrographs of the structure after annealing at 600 and 650°C (Fig. 10). The RBS simulation using RUMP code suggests the formation of Cu oxide at the surface. The XRD result shown in Fig. 3 also supported this oxide formation. The presence of the surface Cu oxide for sample annealed at 500°C could explain the increase in the sheet resistance by ∼200%. The composition of the oxide is determined to be Cu$_2$O from the XRD result.

Fig. 8 shows the RBS spectra for sample **B** (with 20 nm thick Ta) annealed from 350 to 650°C for 35 min. The RBS spectrum for sample **B** annealed at 500°C shows the shifting of the Ta peak to a slightly higher energy. For even higher annealing temperatures, the Ta peak position is shifted back to a lower energy and broadening of the Ta and the Cu peaks were observed. A change in the oxide stoichiometry after 550°C anneal was also observed. The higher sheet resistance measured at 550°C could be attributed to the lost of the conductive Cu layer. The formation of surface Cu$_2$O could result in this lost of conductive Cu layer. The following features were observed for 650°C annealing (i) a significant reduction of the Ta peak height and the broadening of the Ta peak (ii) the tailing of Cu peak into even lower energy. These features indicate a possible formation of a new Cu-Ta compound. The XRD result, shown in Fig. 4, revealed the formation of Cu$_x$Ta$_y$O$_z$ and a significant reduction of Cu peak. The RBS spectra for sample **C** given in Fig. 9 shows very similar phenomena to that for sample **A**. However, the Cu peak annealed at 650°C has a very low intensity (Fig. 5) in the XRD results which indicates an extensive lost of conductive Cu layer, thus giving the highest increase in sheet resistance value as shown in Fig. 2.

Fig. 10 shows the surface morphologies of Cu film after annealing at 600 and 650°C in N$_2$ ambient for 35 min. The grain size of Cu grew as annealing temperature increased but grain growth occurs uniformly. Therefore, it is better described as normal grain growth. Besides grain boundary energy reduction, surface energy and strain energy reductions are the driving forces

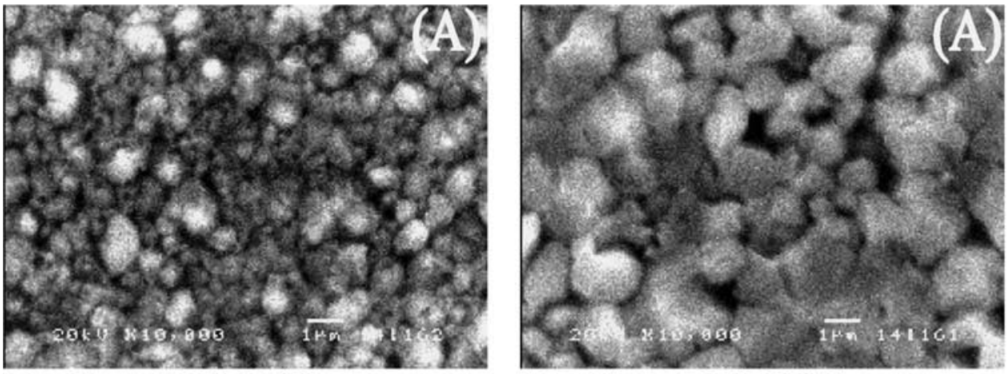

[**A** = 30 nm TaN] 600°C [**A** = 30 nm TaN] 650°C

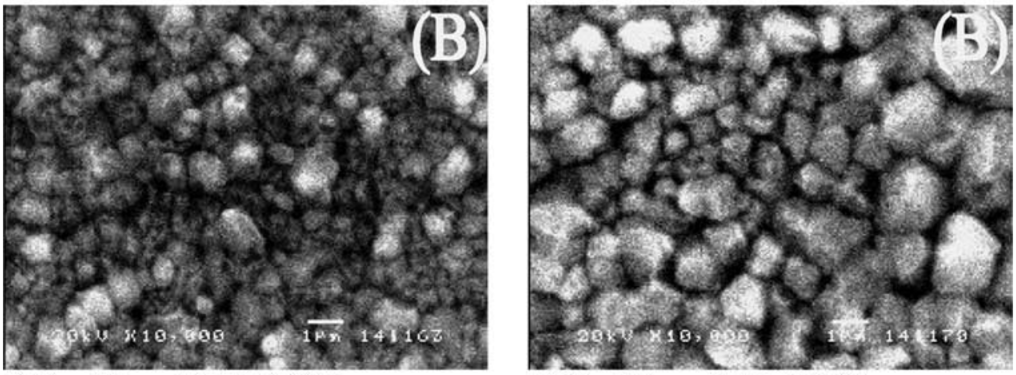

[(**B**) = 20 nm TaN] 600°C [(**B**) = 20 nm TaN] 650°C

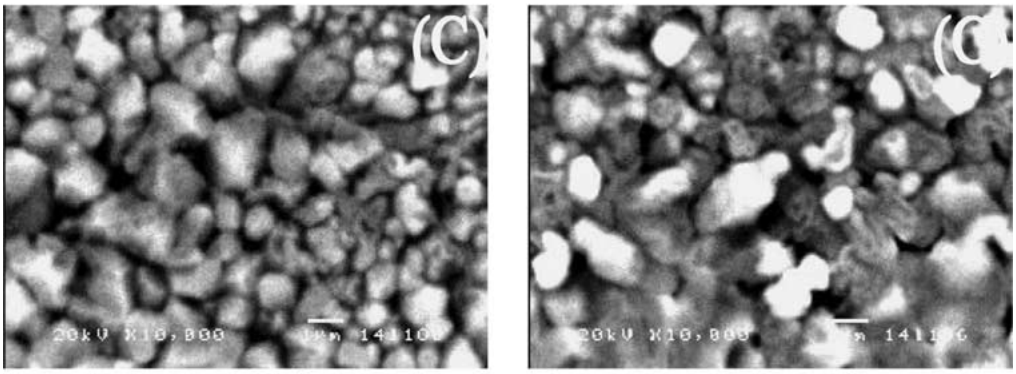

[(**C**)= 10 nm TaN] 600°C [(**C**) = 10 nm TaN] 650°C

Figure 10 SEM micrograph of the Cu/TaN/SiO_2/Si structure after annealing at 600 and 650°C.

for grain growth in thin films [21, 22]. Due to the thin oxide (copper oxides) formed on Cu surfaces, the surface energy of Cu grains or the stress of the film will change, and these variations may cause the accelerated grain growth. It was reported that normal grain growth occurs until the nominal grain size of the film becomes 2–4 times larger than the film thickness, while abnormal grain growth gives a preferential growth of some grains [23, 24]. Zielinski *et al*. reported that if surface energy and stress variation were significantly different with different orientations of grains, some specially oriented grains would grow abnormally to reduce the total system energy. Conversely, if surface energy and stress variation are uniform with the orientation of the grains, abnormal grain growth will not be observed. On the other hand, it is not likely that the uniform variation of surface energy with grain orientation induces the grain growth in thin film [25]. Since the volume of grain boundaries reduces during the grain growth, tensile stress is produced in film. As a consequence, only a compressive stress condition can be relaxed by grain growth [25, 26]. Halliday *et al*. also reported that the oxidation of Cu increased the compressive stress in the film due to the formation of a superficial oxide layer [27]. This suggests the fact that compressive stress induced from the oxidation of Cu becomes the driving forces for the normal grain growth of Cu thin film in our structures.

4. Conclusions

This work investigated the impact of the difference thickness of the TaN diffusion barrier in the Cu/TaN/SiO_2/Si multiplayer structure. Results obtained from high temperatures annealing of the samples pointed out that the property of any thickness of diffusion barriers is mainly deteriorated by their crystallization, out diffusion of Ta towards Cu. TaN layer having an optimal thickness (10 nm) can maintain its integrity the same as higher thickness one (20 and 30 nm). The main compounds observed Cu_2O Ta_2O_5 and $Cu_xTa_yO_z$ were formed due to incorporation of oxygen in the film during deposition and from SiO_2.

References

1. S. P. MURARKA, *Mater. Sci. Eng.* **R19** (1997) 87.
2. A. F. JANKOWASKI, R. M. BIONTA and P. C. GABRIELE, *J. Vac. Sci. Technol. A* **7**(2) (1988) 210.
3. E. KOLAWA and P. M. FRYER, *Appl. Phys. Lett.* **57**(17) (1990) 1736.
4. M. ODA, A. OZAWA, S. OHKI and H. YOSHIHARA, *Jpn. J. Appl. Phys.* **29**(11) (1990) 2616.
5. R. J. GUTMANN, J. M. STEIGERWALD, L. YOU, D. T. PRICE, J. NEIRYNCK, D. J. DUQUETTE and S. P. MURAKA, *Thin Solid Films* **270** (1995) 596.
6. M. H. TSAI, S. C. SUN, C. E. TSAI, S. H. CHAUNG and H. T. CHIU, *J. Appl. Phys.* **79**(9) (1996) 6932.
7. L. A. CLEVENGER, N. A. BOJARCZUK, J. M. E. HAPPER, C. CABRAL Jr., R. G. SCHAD, F. CARDONE and L. STOLT, *ibid.* **73**(1) (1993) 300.
8. M. TAKEYAMA, A. NOYA, T. SASE and A. OHTA, *J. Vac. Sci. Technol. B* **14**(2) (1996) 674.
9. K. HOLLOWAY, P. M. FRYER, C. CABRAL Jr., J. M. E. HARPER, P. J. BAILEY and K. H. KELLEHER, *J. Appl. Phys.* **71**(11) (1992) 5433.
10. K. H. MIN, K. C. CHUN and K. B. KIM, *J. Vac. Sci. Technol. B* **14**(5) (1996) 3263.
11. M. T. WANG, Y. C. LIN and M. C. CHEN, *J. Electrochem. Soc.* **145**(7) (1998) 2538.
12. T. OKU, E. KAWAKAMI, M. UEKUBO, K. TAKAHIRO, S. YAMAGUCHI and M. MURAKAMI, *Appl. Surf. Sci.* **99** (1996) 265.
13. S. M. ROSSNAGEL and J. HOPWOOD, *J. Vac. Sci. Technol. B* **12** (1994) 499.
14. X. SUN, E. KOLAWA, J. S. CHEN, J. S. REID and M. A NICOLET, *Thin Solid Films* **236**(1–2) (1993) 347.
15. K. HIEBER, *ibid.* **24** (1974) 157.
16. M. LANE, R. H. DAUSKARDT, N. KRISHNA and I. HASHIM, *J. Mater. Res.* **15**(1) (2000) 203.
17. K. HOLLOWAY, P. M. FRYER, C. CABRAL, J. M. E. HARPER, P. J. BAILEY and K. H. KELLEHER, *J. Appl. Phys.* **71** (1992) 5433.
18. Y. K. LEE, KHIN MAUNG LATT, KIM JAEHYUNG and KANGSOO LEE, *Journal of Materials Science in Semiconductor Processing*, accepted.
19. P. CHAUDHARI, *J. Vac. Technol.* **9** (1990) 520.
20. H.-J. LEE, K. W. KWON, C. RYU and R. SCINLAIR, *Acta Mater.* **47**(15) (1999) 3965.
21. C. V. THOMPSON, *Scripta Mater. Sci.* **28** (1993) 167.
22. E. Z. ZIELINSKI, R. P. VINCI and J. C. BRAVMAN, *J. Appl. Phys.* **76** (1994) 4516.
23. C. V. THOMPSON, *Annu. Rev. Mater. Sci.* **20** (1990) 245.
24. H. J. FROST, C. V. THOMPSON and D. T. WALTON, *Mater. Sci. Forum* **94–96** (1992) 543.
25. P. CHAUDHARI, *J. Vac. Technol.* **9** (1990) 520.
26. R.-M. KELLER, W. SIGEL, S. P. BAKER, O. KRAFT and E. ARZT, *Mater. Res. Soc. Symp. Proc.* **436** (1997) 221.
27. J. S. HALLIDAY, T. B. RYMER and K. H. R. WRIGHT, *Proc. R. Soc. London A* **225** (1994) 548.

Received 10 October 2000
and accepted 13 July 2001